10468 *Inorg. Chem.* **2010**, *49*, 10468–10474
DOI: 10.1021/ic101502e

Inorganic Chemistry
Article

New Intermetallics $YbAu_2In_4$ and $Yb_2Au_3In_5$

C. Peter Sebastian,[†] James Salvador,[‡] Joshua B. Martin,[§] and Mercouri G. Kanatzidis*[,†]

[†]*Department of Chemistry, Northwestern University, 2145 N. Sheridan Road, Evanston, Illinois 60208, United States,* [‡]*Department of Chemistry, Michigan State University, 320 Chemistry Bldg., East Lansing, Michigan 48824, United States, and* [§]*Functional Properties Group, Ceramics Division, A256 MATLS, National Institute of Standards and Technology (NIST), 100 Bureau Drive, Stop 8520 Gaithersburg, Maryland 20899, United States*

Received July 27, 2010

The intermetallic compounds $YbAu_2In_4$ and $Yb_2Au_3In_5$ were obtained as single crystals in high yield from reactions run in liquid indium. Single crystal X-ray diffraction data of $YbAu_2In_4$ showed that it crystallizes as a new structure type in the monoclinic space group $P2_1/m$ and lattice constants a = 7.6536(19) Å, b = 4.5424(11) Å, c = 9.591(2) Å and β = 107.838(4)°. The $YbAu_2In_4$ compound is composed of a complex $[Au_2In_4]^{3-}$ polyanionic network in which the rare-earth ions are embedded. $Yb_2Au_3In_5$ crystallizes in the polar space group $Cmc2_1$ with the $Y_2Rh_3Sn_5$ type structure and lattice constants a = 4.5351(9) Å, b = 26.824(5) Å, and c = 7.4641(15) Å. The gold and indium atoms define a complex three-dimensional $[Au_3In_5]$ network with a broad range of Au−In (2.751(2) Å−3.0518(16) Å) and In−In (3.062(3) Å−3.3024(19) Å) distances. Magnetic susceptibility measurements of $YbAu_2In_4$ revealed a transition at 25 K. Below the transition, the susceptibility of $YbAu_2In_4$ follows Curie−Weiss behavior with an effective paramagnetic moment of 0.79 μ_B/Yb. Magnetic susceptibility measurements on $Yb_2Au_3In_5$ show a mixed valent ytterbium and the magnetic moment within the linear region (<100 K) of 1.95 μ_B/Yb. Heat capacity data for $YbAu_2In_4$ and $Yb_2Au_3In_5$ give Debye temperatures of 185 and 153 K, respectively.

Introduction

Recent studies have shown that the RE/T/In (RE = Ce, Eu, and Yb and T = transition metal) class of compounds can show interesting physical phenomena arising from competition associated with mixed valency effects. Some notable examples of mixed valent compounds are CeRhIn,[1] and $YbCu_4In$.[2] A brief review on the various structure types of rare-earth−3d transition metal−indium compounds was given by Kalychak.[3] Considerable work has been carried out on compounds with iron, cobalt, nickel, and copper as the transition metal component. Structural elements of these indides include two- or three-dimensional transition metal−indium polyanions, in which the rare-earth atoms separate polyanionic layers and are embedded in channels of a three-dimensional $[T_xIn_y]$ network. Some notable rare earth indides with 3d transition metals are $Ce_4Ni_7In_8$,[4] $CeCu_{4.38}In_{1.62}$,[5] $LaNi_3In_6$,[6] $CeNiIn_4$,[7] $Ho_{10}Ni_9In_{20}$,[8] $Sm_2Co_9In_3$,[9] and $Nd_5Ni_6In_{11}$.[10] Corbett and co-workers have reported a few alkali/alkaline earth-transition metal-indides.[11−22] Recently, we have reported a series of $REAu_2In_4$ compounds with RE = La, Ce, Pr, Nd.[23] All members adopt an orthorhombic structure in the space group *Pnma*. These compounds are polar intermetallic phases composed of a complex $[Au_2In_4]^{3-}$ polyanionic network in which the rare-earth ions are

*To whom correspondence should be addressed. E-mail: m-kanatzidis@northwestern.edu. Phone: 847-467-1541. Fax: 847-491-5937.

(1) Adroja, D. T.; Malik, S. K.; Padalia, B. D.; Vijayaraghavan, R. *Phys. Rev. B* **1989**, *39*, 4831–4833.
(2) Nowik, I.; Felner, I.; Voiron, J.; Beille, J.; Najib, A.; Lachiesserie, E. d. T. d.; Gratz, E. *Phys. Rev. B* **1988**, *37*, 5633–5638.
(3) Kalychak, Y. M. *J. Alloys Compd.* **1997**, *262*, 341–345.
(4) Baranyak, V. M.; Kalychak, Y. M.; Bruskov, V. A.; Zavalii, P. Y.; Dmytrakh, O. V. *Kristallografiya* **1988**, *33*, 601–604.
(5) Kalychak, Y. M.; Baranyak, V. M.; Belsky, V. K.; Dmytrakh, O. V. *Dopo. Akad. Nauk Ukr. Rsr, Seriya B: Geologichni, Khimichni Ta Biologichni. Nauki* **1988**, 39–42.
(6) Kalychak, Y. M.; Gladyshevsky, E. I.; Bodak, O. I.; Dmytrakh, O. V.; Kotur, B. Y. *Kristallografiya* **1985**, *30*, 591–593.
(7) Pöttgen, R. *J. Mater. Chem.* **1995**, *5*, 769–772.
(8) Zaremba, V. I.; Belsky, V. K.; Kalychak, Y. M.; Pecharsky, V. K.; Gladyshevsky, E. I. *Dopo. Akad. Nauk Ukr. Rsr, Seriya B: Geologichni, Khimichni Ta Biologichni. Nauki* **1987**, 42–45.
(9) Baranyak, V. M.; Kalychak, Y. M.; Zavalii, P. Y. *Kristallografiya* **1993**, *38*, 268–270.
(10) Pöttgen, R.; Hoffmann, R. D.; Kremer, R. K.; Schnelle, W. *J. Solid State Chem.* **1999**, *142*, 180–186.
(11) Palasyuk, A. M.; Corbett, J. D. *Inorg. Chem.* **2008**, *47*, 9344–9350.
(12) Palasyuk, A.; Dai, J. C.; Corbett, J. D. *Inorg. Chem.* **2008**, *47*, 3128–3134.
(13) Palasyuk, A.; Corbett, J. D. *Z. Anorg. Allg. Chem.* **2007**, *633*, 2563–2567.
(14) Lin, Q. S.; Corbett, J. D. *J. Am. Chem. Soc.* **2007**, *129*, 6789–6797.
(15) Lin, Q. S.; Corbett, J. D. *Inorg. Chem.* **2007**, *46*, 8722–8727.
(16) Li, B.; Corbett, J. D. *Inorg. Chem.* **2007**, *46*, 6022–6028.
(17) Li, B.; Corbett, J. D. *Inorg. Chem.* **2007**, *46*, 8812–8818.
(18) Dai, J. C.; Corbett, J. D. *Inorg. Chem.* **2007**, *46*, 4592–4598.
(19) Li, B.; Corbett, J. D. *J. Am. Chem. Soc.* **2006**, *128*, 12392–12393.
(20) Li, B.; Corbett, J. D. *Inorg. Chem.* **2006**, *45*, 8958–8964.
(21) Klem, M. T.; Corbett, J. D. *Inorg. Chem.* **2005**, *44*, 5990–5995.
(22) Liu, S. F.; Corbett, J. D. *Inorg. Chem.* **2004**, *43*, 4988–4993.
(23) Salvador, J. R.; Hoang, K.; Mahanti, S. D.; Kanatzidis, M. G. *Inorg. Chem.* **2007**, *46*, 6933–6941.

 Published on Web 10/20/2010

embedded. The $[Au_2In_4]^{3-}$ network features In tetramer units, which defines the compounds as polyindides.

Considerable attention has also been given to systems of the type Yb/M/In, where M is a coinage metal such as Cu, Ag, or Au, which exhibit anomalous valence fluctuations and heavy fermion behavior. Of particular interest is the series $Yb_{0.4}In_{0.6}Cu_2$[24,25] which, together with their Ag and Au analogues,[26] display temperature induced first order valence fluctuations from Yb^{3+} to Yb^{2+} as well as a pressure induced valence transition.[27,28]

Only a few Yb−Au−In compounds have been studied for their crystal structure and physical properties. YbAuIn crystallizes in the ZrNiAl structure type, hexagonal, $P\bar{6}2m$ space group.[29] $YbAu_2In$ (Cubic, $Fm\bar{3}m$, $MnCuAl_2$ type structure) is an intermediate valence compound that shows a pressure induced transition from intermediate valence to trivalent magnetic states.[30] One other example in this family is Yb_2Au_2In, which crystallizes in the Mo_2FeB_2 structure type.[31] Magnetic, resistivity, and specific heat measurements revealed no magnetic ordering for Yb_2Au_2In and divalent Yb. $YbAuIn_2$ crystallizes with the $MgCuAl_2$-type structure (space group *Cmcm*), a ternary ordered version of the Re_3B type.[32] One motivation for the work described here is the continued development of the intermetallic chemistry of Yb and the deeper understanding of its ability to adopt different or mixed oxidation states.

Here we report two new indium rich members of the Yb−Au−In system, $YbAu_2In_4$ and $Yb_2Au_3In_5$. The syntheses of both compounds using the indium flux and high frequency (HF) induction heating methods are detailed. $YbAu_2In_4$ crystallizes in a new crystal structure type and $Yb_2Au_3In_5$, which shares several fundamental structural units with $YbAu_2In_4$, adopts a known but rare polar structure. A structural comparison between $YbAu_2In_4$ and the related isostoichiometric $REAu_2In_4$ (RE = trivalent rare earth element) family is discussed. The inability of the Yb analogue to adopt the RE-Au_2In_4 structure type is consistent with the strong preference of Yb to adopt predominantly a 2+ state. Magnetic susceptibility and heat capacity studies on both compounds were performed, and we find that $YbAu_2In_4$ exhibits a magnetic transition that is associated with a Yb^{2+} to Yb^{3+} valence change.

Experimental Section

Reagents. The following reagents were used as purchased without further purification. Yb (metal chunk, 99.9%, Chinese Rare Earth Information Center, Inner Mangolia, China), Au (pieces, 99.9% Alfa Aesar, Ward Hill, MA), and In (tear drops 99.99% Cerac, Milwauke, WI).

Flux Synthesis of $YbAu_2In_4$. One mmol Yb metal, 3 mmol Au and 15 mmol In were combined in an Al_2O_3 crucible which was then flame-sealed under a reduced atmosphere of 10^{-4} mbar in a fused silica tube. The reactants were heated to 1000 °C over the course of 12 h and held there for 72 h, before cooling down to room temperature over the course of 48 h. Crystals of $YbAu_2In_4$ grow in indium flux generally as metallic silver rods, and the size of the crystals are approximately $2.5 \times 1 \times 0.5$ mm.

Flux Synthesis of $Yb_2Au_3In_5$. For $Yb_2Au_3In_5$, 3 mmol of the Yb metal, 2 mmol Au, and 15 mmol In were combined in an Al_2O_3 crucible which was then flame-sealed under a reduced atmosphere of 10^{-4} mbar in a fused silica tube. The reactants were heated to 1000 °C over 10 h, maintained at that temperature for 5 h to allow proper homogenization, followed by cooling to 850 °C in 2 h and held there for 48 h. Finally, the system was allowed to slowly cool to 50 °C in 48 h. The typical size of the $Yb_2Au_3In_5$ rod-shaped crystals of $2 \times 0.5 \times 0.5$ mm obtained from the synthesis.

The reaction products obtained from both reactions were isolated from the excess indium flux by heating to 350 °C and subsequent centrifugation through a coarse frit. Any remaining flux was removed by immersion and sonication in glacial acetic acid for 48 h. The final crystalline product was rinsed with water and dried with acetone. Several crystals, which grow as metallic silver rods, were carefully selected for elemental analysis, structure characterization, and physical property measurements. The acetic acid did not etch the product noticeably, though the surface of some crystals, especially in the case of $YbAu_2In_4$, were gold coated by etch.

High Frequency Induction Heating. $YbAu_2In_4$. Several attempts to make $YbAu_2In_4$ by direct combination of the elements failed to yield the monoclinic phase when using either the flux heating profile or when increasing the reaction time to one week. Instead, an as yet unidentified phase or phases were produced. The product was a pellet indicating a good melt. Reactions run in a radio frequency induction furnace or an arc welter also did not yield the target phase, but instead formed YbAuIn and an In rich AuIn binary. This system presents another example where molten indium was able to stabilize a phase that could not be synthesized by other methods.

$Yb_2Au_3In_5$. $Yb_2Au_3In_5$ could be synthesized by the high frequency induction heating method. Ytterbium, gold, and indium were mixed in the ideal 2:3:5 atomic ratio and sealed in tantalum ampules under an argon atmosphere in an arc-melting apparatus. The tantalum ampules were subsequently placed in a water-cooled sample chamber of an induction furnace (EasyHeat induction heating system, Model 7590), rapidly heated to about 1000 K and kept at that temperature for 10 min. Finally, the temperature was lowered to 800 K, and the sample was annealed at that temperature for another 30 min. The reaction was then quenched by switching off the power supply. The brittle product could easily be separated from the tantalum tube. No reaction with the ampule was observed.

Elemental Analysis. Quantitative microprobe analyses of $YbAu_2In_4$ and $Yb_2Au_3In_5$ compounds were performed with a Hitachi S-3400 scanning electron microscope (SEM) equipped with a PGT energy dispersive X-ray analyzer. Data were acquired with an accelerating voltage of 20 kV and a 60 s accumulation time. The EDS analyses taken on visibly clean surfaces of the samples gave atomic compositions in good agreement with the results derived from the single crystal X-ray diffraction (XRD) refinements.

Powder XRD. Phase identity and purity of $YbAu_2In_4$ and $Yb_2Au_3In_5$ were determined by powder XRD experiments that were carried out on an Inel diffractometer using Cu Kα radiation. Experimental powder patterns were compared to patterns

(24) Felner, I.; Nowik, I.; Vaknin, D.; Potzel, U.; Moser, J.; Kalvius, G. M.; Wortmann, G.; Schmiester, G.; Hilscher, G.; Gratz, E.; Schmitzer, C.; Pillmayr, N.; Prasad, K. G.; Dewaard, H.; Pinto, H. *Phys. Rev. B* **1987**, *35*, 6956–6963.
(25) Nowik, I.; Felner, I.; Voiron, J.; Beille, J.; Najib, A.; Delacheisserie, E. D.; Gratz, G. *Phys. Rev. B* **1988**, *37*, 5633–5638.
(26) Sarrao, J. L.; Immer, C. D.; Fisk, Z.; Booth, C. H.; Figueroa, E.; Lawrence, J. M.; Modler, R.; Cornelius, A. L.; Hundley, M. F.; Kwei, G. H.; Thompson, J. D.; Bridges, F. *Phys. Rev. B* **1999**, *59*, 6855–6866.
(27) Debray, D.; Werner, A.; Decker, D. L.; Loewenhaupt, M.; Hollandmoritz, E. *Phys. Rev. B* **1982**, *25*, 3841–3845.
(28) Tang, J.; Kosaka, T.; Matsumura, T.; Matsumoto, T.; Mori, N.; Suzuki, T. *Solid State Commun.* **1996**, *100*, 571–574.
(29) Rossi, D.; Ferro, R.; Contardi, V.; Marazza, R. *Z. Metallkd.* **1977**, *68*, 493–494.
(30) Besnus, M. J.; Kappler, J. P.; Ravet, M. F.; Meyer, A.; Lahiouel, R.; Pierre, J.; Siaud, E.; Nieva, G.; Sereni, J. *J Less-Common Met.* **1986**, *120*, 101–112.
(31) Giovannini, M.; Bauer, E.; Michor, H.; Hilscher, G.; Galatanu, A.; Saccone, A.; Rogl, P. *Intermetallics* **2001**, *9*, 481–485.
(32) Galadzhun, Y. V.; Hoffmann, R. D.; Kotzyba, G.; Kunnen, B.; Pöttgen, R. *Eur. J. Inorg. Chem.* **1999**, 975–979.

Table 1. Crystal Data and Structure Refinement for $YbAu_2In_4$ and $Yb_2Au_3In_5$ at Room Temperature

formula	$YbAu_2In_4$	$Yb_2Au_3In_5$
formula weight	1026.25	1511.08
crystal system	monoclinic	orthorhombic
space group	$P2_1/m$	$Cmc2_1$
a/Å	7.6536(19)	4.5351(9)
b/Å	4.5424(11)	26.824(5)
c/Å	9.591(2)	7.4641(15)
α/deg	90.00	90.00
β/deg	107.838(4)	90.00
γ/deg	90.00	90.00
Z	2	4
V/Å^3	317.41(13)	908.0(3)
ρ/gcm^{-3}	10.738	11.054
μ/mm^{-1}	74.741	80.990
F(000)	848	2488
reflections collected	3939	3995
unique data	1079	1349
R_{int}	0.0501	0.0732
parameters	44	63
$R_1{}^a$ [$I > 2\sigma(I)$]	0.0436	0.0404
$wR_2{}^b$	0.1182	0.1144

^{a} $R_1 = \sum||F_o| - |F_c||/\sum|F_o|$. ^{b} $wR_2 = \{\sum w(F_o{}^2 - F_c{}^2)^2/\sum w(F_o{}^2)^2\}^{1/2}$ and $w = 1/(\sigma^2(I) + 0.0016I^2)$.

calculated from the structural refinement. The powder XRD patterns of both compounds were in good agreement with the simulated patterns.

Single Crystal XRD. $YbAu_2In_4$. Single crystal XRD data were collected at room temperature using a Bruker AXS SMART CCD diffractometer with graphite monochromatized Mo Kα (λ = 0.71073 Å) radiation. Unit cell refinement and data merging were done with the SAINT program, and an empirical absorption correction was applied using the program SADABS.[33] The original determination of the unit cell of $YbAu_2In_4$ lead to a monoclinic cell with lattice parameters a = 7.6536 (19) Å, b = 4.5424 (11) Å, c = 9.591 (2) Å, and β = 107.838(4)°. No hkl extinction condition was found, indicating the cell was primitive. The program XPREP was used to determine the space group. The only systematic absence was the $0k0$, $k = 2n$, which yielded two possible space groups $P2_1$ and $P2_1/m$. A stable refinement was accomplished in the centrosymmetric space group.

$Yb_2Au_3In_5$. The X-ray intensity data were collected at room temperature using a STOE IPDS 2T (with additional capability of 2θ swing of the detector) diffractometer with graphite-monochromatized Mo Kα (λ = 0.71073 Å) radiation. The X-AREA (X-RED and X-SHAPE within) package suite[34] was used for the data extraction and integration and to apply empirical and analytical absorption corrections. The structure was solved by direct methods and refined with the SHELXTL package of programs.[35] A stable refinement for $Yb_2Au_3In_5$ was accomplished only in the orthorhombic space group $Cmc2_1$ and $Y_2Rh_3Sn_5$ structure type.

The details of the data collection and crystallographic refinement of $YbAu_2In_4$ and $Yb_2Au_3Sn_5$ are given in Table 1. A list of the atomic positions, isotropic displacement parameters, and the anisotropic displacement parameters are available in the Supporting Information. The bond distances can be found in Table 2 and Table 3 for $YbAu_2In_4$ and $Yb_2Au_3In_5$, respectively.

Magnetic Measurements. Magnetic measurements of $YbAu_2In_4$ and $Yb_2Au_3In_5$ were carried out on a Quantum Design MPMS SQUID magnetometer. Measurements were performed on hand selected single crystals, which were ground and screened by powder XRD to verify phase identity and purity. Temperature dependent data were collected for both zero field cooled (ZFC) and field cooled mode (FC) between 2 and 300 K with an applied field of 1 kG. Magnetization data were also collected for $YbAu_2In_4$ at 5 K with field sweeping from −55 kOe to 55 kOe. A diamagnetic correction was applied to the data to account for the core diamagnetism.

Heat Capacity. Temperature dependent heat capacity (C_p) of $YbAu_2In_4$ and $Yb_2Au_3In_5$ was measured in the range 5−300 K using a commercial Quantum Design Physical Property Measurement System (QD-PPMS) (The purpose of identifying the equipment in this article is to specify the experimental procedure. Such identification does not imply recommendation or

Table 2. Bond Lengths [Å] for $YbAu_2In_4$ with Estimated Standard Deviations in Parentheses

label	distance	label	distance
Yb−Au(2) × 2	3.3039(10)	In(1)−In(2)	2.917(2)
Yb−In(4) × 2	3.3053(13)	In(1)−In(4)	3.101(2)
Yb−In(1) × 2	3.3156(13)	In(1)−In(1) × 2	3.2795(19)
Yb−In(2)	3.3336(18)	In(1)−Yb × 2	3.3156(13)
Yb−In(2) × 2	3.3391(12)	In(1)−Yb	3.4093(17)
Yb−Au(1) × 2	3.3610(10)	In(2)−Au(2) × 2	2.7957(10)
Yb−In(1)	3.4093(17)	In(2)−Au(2)	2.8972(17)
Au(1)−In(1) × 2	2.8067(10)	In(2)−In(3)	3.290(2)
Au(1)−In(4) × 2	2.8243(10)	In(2)−In(2) × 2	3.308(2)
Au(1)−In(4)	2.8306(16)	In(2)−Yb	3.3336(18)
Au(1)−In(1)	2.8421(16)	In(2)−Yb × 2	3.3391(12)
Au(1)−In(3)	2.8680(16)	In(3)−Au(2) × 2	2.9647(11)
Au(1)−Yb × 2	3.3610(10)	In(3)−In(3) × 2	3.314(2)
Au(2)−In(4)	2.7869(16)	In(3)−In(4) × 2	3.3156(15)
Au(2)−In(2) × 2	2.7957(10)	In(3)−Yb	3.5994(18)
Au(2)−In(3)	2.8070(16)	In(4)−Au(1) × 2	2.8243(10)
Au(2)−In(2)	2.8972(17)	In(4)−Au(1)	2.8306(16)
Au(2)−In(3) × 2	2.9647(11)	In(4)−Yb	3.3053(13)
Au(2)−Yb	3.3039(10)	In(4)−In(3) × 2	3.3156(15)
In(1)−Au(1) × 2	2.8068(10)	In(4)−In(4) × 2	3.341(2)
In(1)−Au(1)	2.8422(16)	In(4)−Yb	3.4895(16)

Table 3. Bond Lengths [Å] for $Yb_2Au_3In_5$ with Estimated Standard Deviations in Parentheses

label	distances	label	distances
Yb(1)−Au(3)	3.1954(13)	Au(1)−Yb(2)	3.2860(14)
Yb(1)−Au(3)	3.1954(13)	Au(2)−In(2)	2.7860(15)
Yb(1)−In(5)	3.2562(19)	Au(2)−In(2)	2.7860(15)
Yb(1)−In(5)	3.2562(19)	Au(2)−In(2)	2.786(2)
Yb(1)−In(2)	3.2778(18)	Au(2)−In(5)	2.7944(14)
Yb(1)−In(2)	3.2778(18)	Au(2)−In(5)	2.7944(15)
Yb(1)−In(4)	3.377(2)	Au(2)−In(1)	2.833(2)
Yb(1)−In(3)	3.4037(19)	Au(2)−In(5)	2.849(2)
Yb(1)−In(3)	3.4037(19)	Au(2)−Yb(1)	3.4373(13)
Yb(1)−Au(2)	3.4374(13)	Au(2)−Yb(1)	3.4373(13)
Yb(1)−Au(2)	3.4374(13)	Au(3)−In(2)	2.751(2)
Yb(1)−In(2)	3.448(3)	Au(3)−In(4)	2.8096(14)
Yb(2)−Au(3)	3.0296(18)	Au(3)−In(4)	2.8096(14)
Yb(2)−Au(1)	3.1679(12)	Au(3)−In(3)	2.898(2)
Yb(2)−Au(1)	3.1679(12)	Au(3)−In(1)	3.0518(16)
Yb(2)−In(4)	3.2660(16)	Au(3)−In(1)	3.0518(16)
Yb(2)−In(4)	3.2660(16)	Au(3)−Yb(1)	3.1954(13)
Yb(2)−Au(1)	3.2860(13)	Au(3)−Yb(1)	3.1954(13)
Yb(2)−Au(1)	3.2860(13)	In(1)−Au(1)	2.855(2)
Yb(2)−In(3)	3.371(3)	In(1)−Au(3)	3.0518(16)
Yb(2)−In(3)	3.462(3)	In(1)−Au(3)	3.0518(16)
Yb(2)−In(4)	3.4763(19)	In(1)−In(4)	3.243(3)
Yb(2)−In(4)	3.4763(19)	In(1)−Yb(2)	3.554(2)
Yb(2)−In(1)	3.554(2)	In(1)−Yb(2)	3.554(2)
Au(1)−In(4)	2.768(2)	In(1)−Yb(1)	3.708(3)
Au(1)−In(3)	2.7766(14)	In(2)−Au(2)	2.7860(15)
Au(1)−In(3)	2.7766(14)	In(2)−Au(2)	2.7860(15)
Au(1)−In(1)	2.855(2)	In(2)−Au(2)	2.786(2)
Au(1)−In(4)	2.872(2)	In(2)−In(5)	3.062(3)
Au(1)−Yb(2)	3.1679(13)	In(2)−Yb(1)	3.2778(18)
Au(1)−Yb(2)	3.1679(13)	In(2)−Yb(1)	3.2778(18)
Au(1)−Yb(2)	3.2860(14)	In(2)−In(5)	3.3024(19)

(33) Sheldrick, G. M. *SADABS*; University of Göttingen: Göttingen, Germany.
(34) *X-Area*; Cie STOE & Cie GmbH: Darmstadt, Germany, 2006.
(35) Sheldrick, G. M. *SHELXS-97, Program for the solution of crystal structure*; University of Göttingen: Göttingen, Germany, 1997.

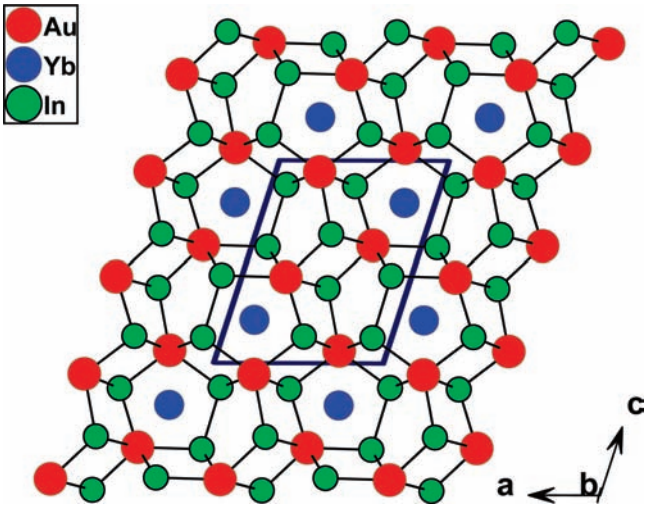

Figure 1. Structure of $YbAu_2In_4$ as viewed along the *b*-axis with the unit cell outlined.

endorsement by the National Institute of Standards and Technology). The data were obtained under standard thermal relaxation methods in a zero magnetic field. Thermal coupling between each sample and the sample platform was achieved via Apiezon N grease, and the sample platform coupled to the sample puck via thin wires. Conduction through these wires is the dominant mode of thermal transfer, enabled by cryopumping the chamber below 1.3×10^{-5} Pa. Prior to each sample measurement, the sample puck, platform, and the Apiezon N grease were thoroughly characterized in a separate addenda measurement.

Results and Discussion

Structure. $YbAu_2In_4$. The crystal structure of $YbAu_2In_4$ is shown in Figure 1. $YbAu_2In_4$ exhibits a new structure type but has similar building units to other *RE*−Au-In compounds. The distribution of gold atoms in $YbAu_2In_4$ is similar to that of $REAu_2In_4$, presented previously,[23] featuring Au_2In_2 parallelograms and no Au−Au contacts. The Au_2In_2 rhombic parallelogram is a common feature of *RE*−Au-In systems which is most likely a result of the Au atoms being the most electronegative elements in the structure and thus electrostatically repulsed. These parallelograms condense to form a complex three-dimensional Au/In polyanion. In $REAu_2In_4$ (*RE* = La, Ce, Pr, and Nd), Au_2In_2 parallelograms condense as edge sharing units along the *a*-axis and connect along common Au atoms along the *c*-axis.[23] We see that a similar configuration exists for $YbAu_2In_4$, in that the Au_2In_2 units are condensed to form edge-sharing ribbons along the *c*-axis and these ribbons are connected via corner sharing units along the *a*-axis. This arrangement is depicted in the wire frame structure of $YbAu_2In_4$ and $REAu_2In_4$ shown in Figure 2. The main difference between these structures is the connectivity of the In sublattice. In $REAu_2In_4$, the In atoms form isolated tetramers, which interpenetrate and propagate along the *b*-axis, while $YbAu_2In_4$ contains only In dimers formed by In(1) and In(2) with a distance of 2.917(2) Å. The remaining In distances are well over 3.2 Å and are too long to be considered strong bonding interactions.[36]

(36) Pauling, L. *The Nature of the Chemical Bond*; Cornell University Press: Ithaca, NY, 1968.

Figure 3 shows the bonding environment of the Yb, Au(1), and Au(2) atoms of $YbAu_2In_4$. The coordination geometry of ytterbium is a tricapped pentagonal prism with one indium and two gold capping atoms. On the other hand, the coordination geometry for both Au atoms is tricapped trigonal prism. The prism around Au(1) is capped by one indium and two ytterbium atoms, whereas Au(2) is capped by three indium atoms. Yb is coordinated by four Au and seven In. The two Yb−Au(1) bond distances are 3.3610(10) Å and the two Yb−Au(2) distances are 3.3039(10) Å. In(1) forms two bonds at 3.315(1) Å and In(2) forms three bonds, two at 3.339(1) Å and the third at 3.333(2) Å. In(4) forms the final two bonds with a distance of 3.3053(12) Å. As was the case in $REAu_2In_4$, the two crystallographically distinct Au atoms of $YbAu_2In_4$ have nearly identical bonding environments, that is, both are bound to seven surrounding In atoms.

$Yb_2Au_3In_5$. $Yb_2Au_3In_5$ crystallizes in the $Y_2Rh_3Sn_5$ type structure.[37] Thus far, there are three different types of $RE_2T_3X_5$ compounds that have been observed. All are orthorhombic with slight differences in their crystal structures. The first, $Y_2Rh_3Sn_5$ type,[37] crystallizes in $Cmc2_1$, and its reported isotypic compounds are $RE_2Rh_3Sn_5$ (*RE* = Ce−Nd, Sm, Gd−Tm),[37] $Ce_2Rh_3(Pb,Bi)_5$[38] and $Eu_2Pt_3Sn_3$.[39] The second, $Yb_2Pt_3Sn_5$, crystallizes in *Pnma*[40] and is adopted by $Ca_2Pt_3Sn_5$[41] and $CaREPt_3Sn_5$ (*RE* = Er−Lu).[42] $Ce_2Au_3In_5$ is the third type ($Pmn2_1$) that is adopted by $RE_2Au_3In_5$ (*RE* = Ce, Pr, Nd, Sm).[43] The structural relationships of these three types have been discussed in detail by Kussmann et al.[42]

The structure of the $Y_2Rh_3Sn_5$ type compounds has been discussed in detail.[37−39] As shown in Figure 4, the structure of $Yb_2Au_3In_5$ is built of two-dimensional Au−In rings stacked along the *a*-direction, which encapsulate Yb atoms in the three-dimensional channels. The structure of $Yb_2Au_3In_5$ can also be explained as the interconnection of Au_2In_2 rhombic parallelograms. Similar to the other Yb−Au−In compounds and as we explained for $YbAu_2In_4$, there are no Au−Au contacts but instead the Au atom occupies the opposite side of the parallelogram. However, the arrangement of the parallelogram is different in $Yb_2Au_3In_5$, where along [100] two such parallelograms are condensed through their edges, Figure 4. These double parallelograms are condensed via edge sharing with other doubles and singles in the *bc* plane. Another interesting feature of this structure, which was not highlighted for other $Y_2Rh_3Sn_5$ type compounds, is the presence of two different types of layers. One is slightly flat and the second is distorted, and both are formed by Au and In atoms (Figure 5). A

(37) Meotmeyer, M.; Venturini, G.; Malaman, B.; Steinmetz, J.; Roques, B. *Mater. Res. Bull.* **1984**, *19*, 1181–1186.
(38) Thomas, E. L.; Kim, M. S.; Sokolov, D. A.; Bennett, M. C.; Aronson, M. C.; Chan, J. Y. *J. Solid State Chem.* **2007**, *180*, 2356–2362.
(39) Harmening, T.; Hermes, W.; Eul, M.; Schappacher, F. M.; Pöttgen, R. *Z. Kristallogr.* **2009**, *224*, 351–357.
(40) Pöttgen, R.; Lang, A.; Hoffmann, R. D.; Kunnen, B.; Kotzyba, G.; Mullmann, R.; Mosel, B. D.; Rosenhahn, C. *Z. Kristallogr.* **1999**, *214*, 143–150.
(41) Hoffmann, R. D.; Kussmann, D.; Rodewald, U. C.; Pöttgen, R.; Rosenhahn, C.; Mosel, B. D. *Z. Naturforsch., B: Chem. Sci.* **1999**, *54*, 709–717.
(42) Kussmann, D.; Pöttgen, R.; Kotzyba, G. *J. Solid State Chem.* **2000**, *150*, 112–120.
(43) Galadzhun, Y. V.; Hoffmann, R. D.; Pöttgen, R.; Adam, M. *J. Solid State Chem.* **1999**, *148*, 425–432.

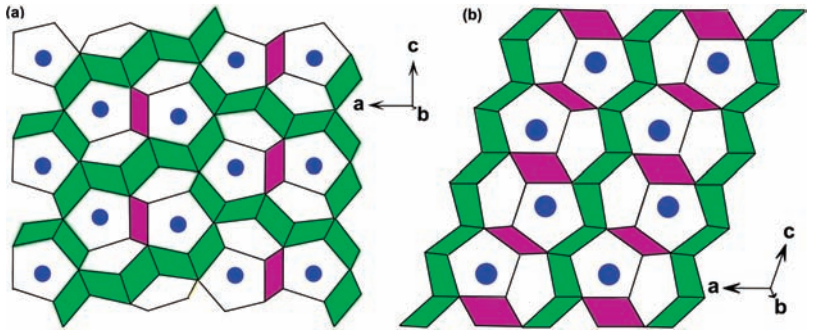

Figure 2. Wire frame view of (a) REAu$_2$In$_4$ (RE = La, Ce, Pr, Nd) and (b) YbAu$_2$In$_4$ with shading of the Au$_2$In$_2$ parallelograms. In REAu$_2$In$_4$, Au$_2$In$_2$ parallelograms are condensed as edge sharing units along the a-axis and corner sharing along common Au atoms along the c-axis. YbAu$_2$In$_4$ is composed of edge sharing parallelograms of Au$_2$In$_2$ propagating along the c-axis and interconnected by corner sharing parallelograms along the a-axis with common Au atoms.

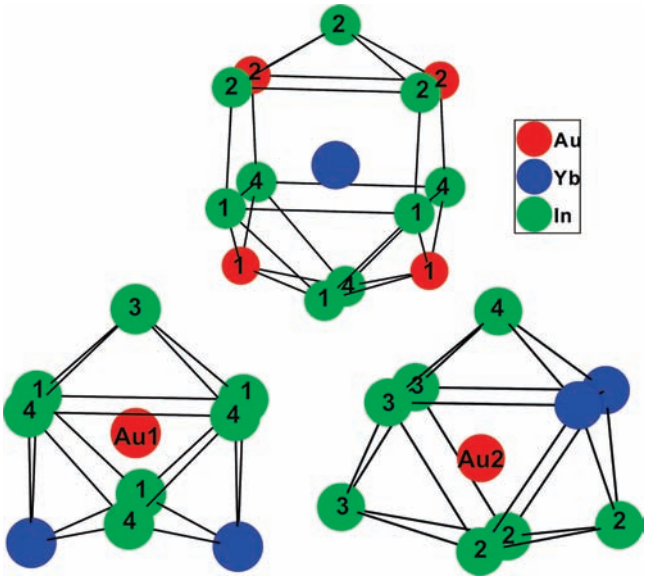

Figure 3. Coordination environment for Yb and Au atoms in YbAu$_2$In$_4$. No atoms are shown that have bond distances longer than 3.5 Å.

different view of the Au$_3$In$_5$ building unit can be seen in this plane. In the flat layer, the building units are condensed via edge sharing along the c-axis and connected with common Au atoms along the a-axis. However, in the distorted layer, the parallelogram sheets along the c-axis are not connected via common Au atoms but are separated by tetrahedral In atoms.

Crystallographically, there are two different Yb sites in Yb$_2$Au$_3$In$_5$, and the coordination environment around each (Figure 6) is significantly different. The Yb1 atoms have a coordination number of 20 with 2 Yb, 7 Au, and 11 In atoms in their coordination shell, but Yb2 atoms have a coordination number of 18 with 4 Yb, 6 Au, and 8 In. The shortest Yb1−Yb1 and Yb2−Yb2 interatomic distances are 4.5351(9) Å and 3.8939(7) Å, respectively. The differences between the two Yb atoms indicate a different valence behavior, and we tentatively assign the larger Yb^{2+} for Yb1 and the smaller Yb^{3+} for Yb2. A similar kind of mixed valency for Yb was also proposed for Yb$_2$Pt$_3$Sn$_5$.[40,44]

Magnetic Measurements. YbAu$_2$In$_4$. Magnetic susceptibility measurements were made on single crystals

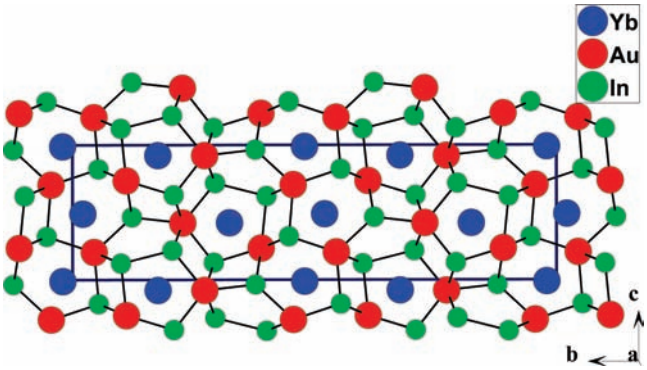

Figure 4. Crystal structure of Yb$_2$Au$_3$In$_5$ as viewed down the a-axis. Bonds to the Yb atoms have been omitted for clarity.

of YbAu$_2$In$_4$ aligned randomly, and the results are shown in Figure 7. From 300 to 160 K, YbAu$_2$In$_4$ displays a negligible temperature independent susceptibility but at ~160 K, it increases slightly until ~125 K and then the weak temperature dependence remains unchanged. A transition is found at 25 K, and the susceptibility dramatically increases over a very small temperature range. The data begin to follow a Curie−Weiss law at this point (Figure 7 inset) with a resulting effective magnetic moment of 0.79 μ_B/Yb atom. This is less than a quarter of the value expected for an Yb^{3+} ion, the only ion expected to make a paramagnetic contribution to the susceptibility.

A possible explanation for this behavior is that the Yb ion is undergoing a valence transition from the diamagnetic Yb^{2+} state with a filled f shell to an intermediate valence state with an oxidation state between 2+ and 3+, therefore becoming paramagnetic. First order valence fluctuations of this type are not unprecedented and have been observed in YbCu$_4$In, where the Yb undergoes an Yb^{3+} to Yb^{2+} transition at 20 K.[24]

The magnetization curve for YbAu$_2$In$_4$, which was measured at 5 K, can be seen in Figure 8. The moment has a nearly linear dependence on the applied field up to 20 kOe, at which point the dependence begins to saturate up to about 40 kOe. This behavior is consistent with essentially a paramagnetic system and is what we would expect based on the proposed valence transition explained above. However, the magnetization seems to saturate at a very small value at high fields implying the possible presence of minor impurities.

(44) Muro, Y.; Yamane, K.; Kim, M. S.; Takabatake, T.; Godart, C.; Rogl, P. *J. Phys. Soc. Jpn.* **2003**, *72*, 1745–1750.

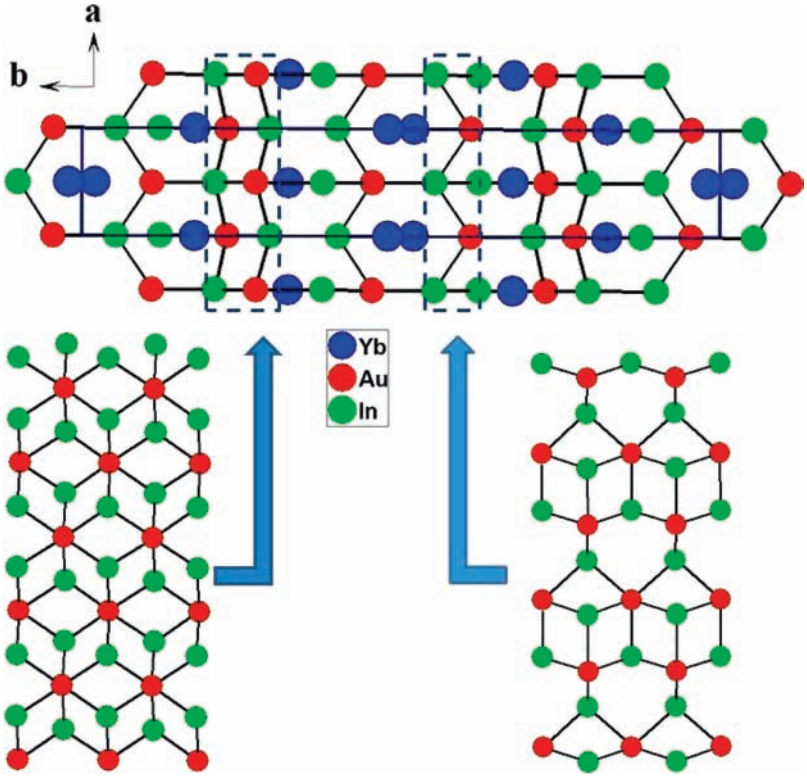

Figure 5. Structure of $Yb_2Au_3In_5$ viewed down the *c*-axis. Two types of Au_3In_5 layers present in $Yb_2Au_3In_5$.

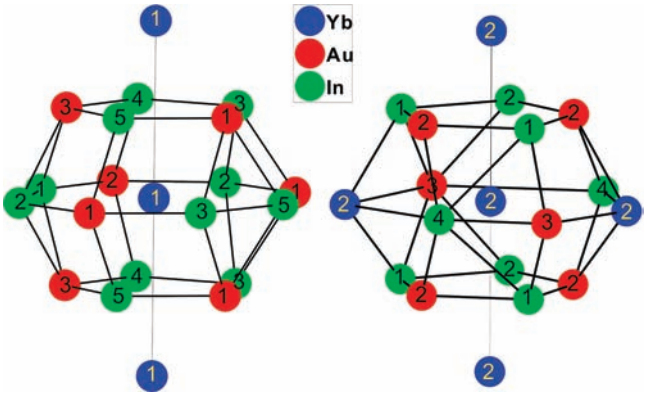

Figure 6. Coordination polyhedra of Yb(1) and Yb(2) atoms in $Yb_2Au_3In_5$. No atoms are shown at distances longer than 3.5 Å.

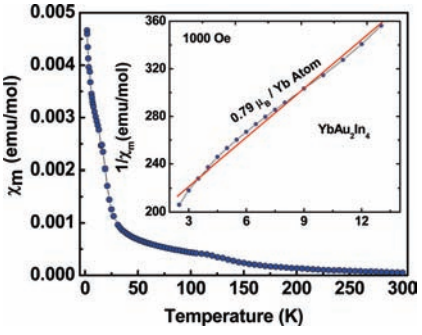

Figure 7. Magnetic susceptibility for a polycrystalline sample of $YbAu_2In_4$ showing a valence transition at 25 K under an applied magnetic field of 1 kOe. Inset figure: inverse susceptibility plot of $YbAu_2In_4$ for data below 14 K.

The valence transition can be explained in terms of the Yb ion responding to physical pressure on the system induced by normal lattice contraction on cooling. This situation can promote the development of Yb^{3+}, which is smaller than Yb^{2+}, and is not unlike those found in Sm and Tm chalcogenide compounds, which undergo RE^{2+} to RE^{3+} transitions with the application of pressure.[27,28,45]

$Yb_2Au_3In_5$. Magnetic susceptibility measurements were performed on a polycrystalline sample of $Yb_2Au_3In_5$ obtained from HF synthesis. The temperature dependent magnetic susceptibility of $Yb_2Au_3In_5$ at an applied field of 1 kOe is shown in Figure 9. The inverse molar magnetic susceptibility data versus temperature is shown as an inset in Figure 9. The temperature dependence of the molar susceptibility (χ_m) indicated paramagnetic behavior and suggests the existence of Yb^{3+} moments in the material. No magnetic ordering was observed down to 2 K. The inverse susceptibility follows the Curie−Weiss law only in the temperature region above 100 K. At lower temperatures the deviation can be attributed to crystal-field contributions and/or to a possible onset of a valence fluctuation. Above 100 K $Yb_2Au_3In_5$ exhibits paramagnetic behavior with an effective moment of 1.95 μ_B/Yb atom. The estimated experimental μ_{eff} value is about 43% of that expected for a free Yb^{3+} ion (4.54 μ_B). The negative Weiss temperature (θ_p) obtained (−223 K) suggests strong antiferromagnetic interactions between the two Yb atoms.

Heat Capacity. The temperature dependent molar specific heat data for $YbAu_2In_4$ and $Yb_2Au_3In_5$ are measured within 5−300 K. Within the Debye approximation

(45) Jayaraman, A.; Narayana, V.; Bucher, E.; Maines, R. G. *Phys. Rev. Lett.* **1970**, *25*, 1430–1433.

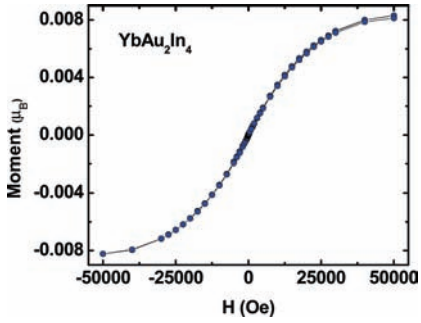

Figure 8. Magnetization curve for a polycrystalline sample of $YbAu_2In_4$ at 5 K as a function of field.

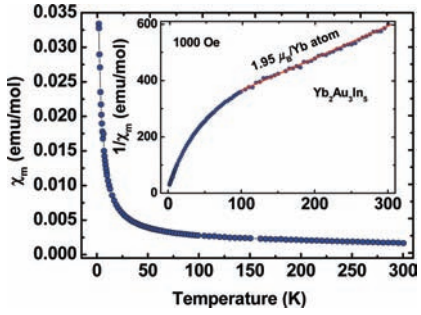

Figure 9. Molar magnetic susceptibility as a function of temperature for a polycrystalline sample of $Yb_2Au_3In_5$ sample measured in a field of 1 kOe. Inset figure: temperature dependent inverse susceptibility of $Yb_2Au_3In_5$. The linear region 100−300 K is marked clearly in the figure.

at low temperature, the measured specific heat is given as

$$C_p = \gamma T + \beta T^3 \quad \text{or} \quad C_p/T = \gamma + \beta T^2 \qquad (1)$$

where, γ is the contribution from the conduction electrons and β is the lattice contribution.[46] As per eq 1, the value of γ is interpreted as the effective mass of electrons at the Fermi surface.

Fitting the $C_p(T)/T$ versus T^2 dependence at low temperature (< 20 K) and extrapolating to $T = 0$ yields an electronic Sommerfeld parameter, γ, of 49 mJ mol^{-1} K^{-2} for $Yb_2Au_3In_5$ and 38 mJ mol^{-1} K^{-2} for $YbAu_2In_4$. The relatively low magnitude of the electronic component (γ) suggests that $YbAu_2In_4$ and $Yb_2Au_3In_5$ are not likely to be heavy-fermion materials according to the arbitrary classification of such compounds into "light", "moderate", and classical heavy-fermions with γ values lying in the range of ~50−60, 100−400, and >400 mJ/mol K^2, respectively. The Debye phonon contribution was also estimated from the fit[46] yielding a value of 2.1×10^{-3} J K^{-4} mol^{-1} for $YbAu_2In_4$ and 5.3×10^{-3} J K^{-4} mol^{-1} for $Yb_2Au_3In_5$, corresponding to a Debye temperature, θ_D, of 185 and 153 K, respectively. The heat capacity does not show the steep rise characteristic corresponding to the magnetic transitions probably because of lattice vibrations. Instead, it is a nearly linear function of the temperature between 5 and 300 K.

(46) Gopal, E. S. R. *Specific heat at low temperatures*; Plenum: New York, 1966.

Concluding Remarks

$YbAu_2In_4$ and $Yb_2Au_3In_5$ are two new compounds in the Yb−Au−In system obtained from In elemental flux. These are the first examples of the reactive behavior of indium flux in the Yb−Au−In ternary system, and their discovery underscores the potential of this flux as a useful synthetic medium for new intermetallic compounds. In both cases, we find that Yb is not in a diamagnetic 2+ state, but a small paramagnetic contribution coming from Yb^{3+} species is clearly present. It is possible the Au, which is a rather electronegative atom, favors the partial oxidation of Yb^{2+} via internal electron transfer. The stability of $YbAu_2In_4$ and $Yb_2Au_3In_5$ and the possible internal redox interplay between Yb and the transition metal motivates further investigations on the existence of analogous compounds with compositions of YbT_2In_4 and $Yb_2T_3In_5$ (T = transition metals) or other indium rich compounds. The valence fluctuation behavior of Yb as a function of T would be of particular interest and could shed further light on how it can be controlled.

Acknowledgment. Financial support from the Department of Energy (Grant DE-FG02-07ER46356) is gratefully acknowledged. Use was made of facilities operated by the Northwestern Materials Research Center under NSF Grant DMR-0520513. Technical support was provided by Dr. O. Chernyashevskyy.

Supporting Information Available: Crystallographic information files (CIF), tables of atomic coordinates and anisotropic displacement parameters, crystal structures with thermal parameters. This material is available free of charge via the Internet at http://pubs.acs.org.